LGBC Silicon Solar Cell with modified bus bar suitable for high volume wire bonding

Keith C Heasman[1], Laura M Brown[1], Alex Cole[1], Stephen Devenport[1], Paul Gibbard[2] and Tim M Bruton[1]
[1]Narec, PV Technology Centre, Albert Street, Blyth, Northumberland, NE24 1LZ, UK
[2] Welwyn Components Ltd, Welwyn Electronics Park, Bedlington, Northumberland, NE22 7AA
[*]*Corresponding Author: keith.heasman@narec.co.uk*

Introduction

Laser Grooved Buried Contact (LGBC) solar cells has been manufactured by Narec since 2005. The front contact bus bar is optimised for contact by continuous soldering an interconnect ribbon along its length. For the APOLLON [1] project (an EU FP7 funded project to develop high concentration Point Focus and Dense Array systems with a final target cost of 2€/W_p), Narec was required to redesign the existing cell to produce an alternative front contact bus bar that would be compatible with more cost effective high volume automated interconnection technology such as ultrasonic welding or wire bonding.
The standard LGBC bus bar is shown in figure 1, it is made up of many grid lines separated by regions of anti-reflection coated silicon between them, a surface that was thought not to be suitable for bonding to.

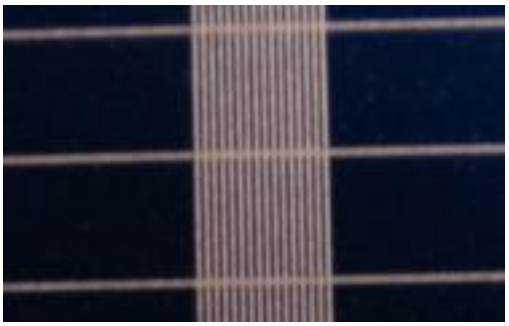

Figure 1: Standard LGBC front bus bar contact.

This paper describes the development and wire bonding performance of the hybrid front contact design of laser grooved grid lines and a solid planar contact bus bar.

Approach

An alternative all LGBC solid bus bar contact was initially produced by reducing the separation of the individual laser grooves in the bus bar and by varying the focus and depth of cut. Instead of grooves separated by 100µm, the distance between the grooves was reduced. After removing the laser damage by etching in an alkaline solution a deep wide trench was created, which following heavy diffusion was electrolessly plated using our standard process. Figure 2 shows an optical microscope image of the bus bar region that is created following the modified laser grooving.

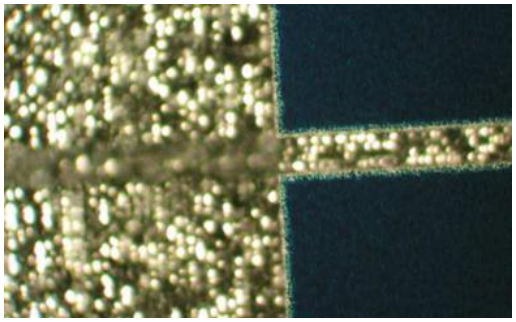

Figure 2: Optical microscope image of a modified continuous solid bus bar.

Figure 3 is an optical interferogram that shows the step in height from the silicon surface down into the bus bar, the mean step height was approximately 20µm, the arithmetic mean surface roughness in the bus bar region was Ra=3µm.

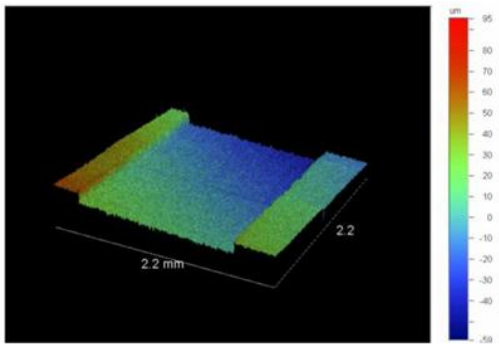

Figure 3: Optical interferogram image of the surface profile across the whole of the modified solid bus bar.

A batch of wafers was run through the Narec LGBC production line to compare standard 1Sun cells with cells incorporating a solid bus bar fabricated using the same parameters as the initial samples. Table 1 shows a summary of the measured solar

cell parameters from this trial. No significant difference was observed between the cell parameters of the standard and solid bus bar cell groups.

Bus Bar type	Mean / Std. Dev	J_{sc} (mA/cm^2)	Voc (mV)	FF (%)	Efficiency (%)	R_s (mΩ)	R_{sh} (Ω)
Standard	Mean	35.12	610.2	79.70	17.09	2.84	42
	Std. Dev.	0.13	1.9	0.3	0.17	0.08	36
Solid	Mean	35.14	611.6	79.83	17.16	2.85	104
	Std. Dev.	0.08	1.0	0.19	0.08	0.13	107

Table 1: Comparison of cell parameters for standard and solid bus bar 1SUN cells measured under standard AM1.5 test conditions

Modified Bus Bar Optimisation

In order to optimise the initial solid bus bar design, a test pattern was used to investigate the main factors contributing to the solid bus bar patterning, namely gap distance between laser grooves, stage speed and laser power.

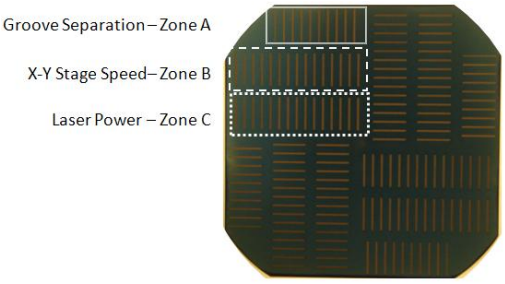

Figure 4: Test pattern for investigation of the parameters influencing solid bus bar patterning.

The 3-Zone-test pattern shown in figure 4 was replicated 4 times across the wafer to include spatial effects and laser scribe direction although neither of these proved to be significant. The first optimisation trial with the test pattern concluded that laser power, speed of the X-Y table movement and groove separation distance all influence the appearance of the solid bus bar after etching of the damaged region to one degree or another. Laser power in particular changes the surface roughness. The additional laser time incurred to produce the solid bus bar can be offset by an increase in the laser cutting speed without influencing the appearance significantly.

Initial experimental assessment was carried out by optical inspection of the resultant surface. Figure 5 shows microscope images from the zone A experiment designed to establish which X-Y stage movement was required to produce a single merged trench rather than standard single grooves. High magnification of the 0.024mm spacing shows that the groove ridges are still seen but with a gap of 0.018mm the grooves are sufficiently overlapped that only the surface roughness of the bottom of the trench can be seen. Also it was observed that standard wet etch cleaning conditions provided sufficient laser debris removal even in the smallest gap width samples.

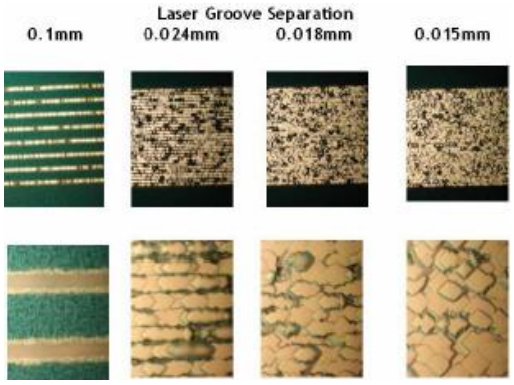

Figure 5: High magnification images of the laser groove separation experiment (Zone A) after wet etching.

Figure 6 shows zone B results where the speed of the laser stage was varied to observe the affect on surface roughness. As expected faster movement resulted in slightly more residual grooving i.e. a line can still be seen slightly on the fastest samples. This can be removed by reducing the gap size further. As no negligible trench depth difference is seen in the faster samples the affect on throughput of patterning the additional grooves can be offset by stage speed adjustment.

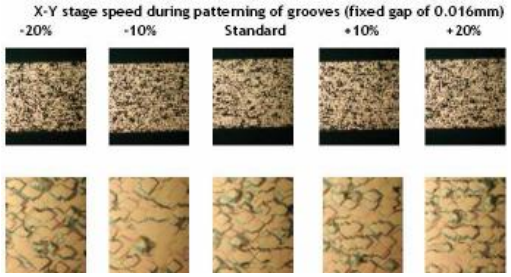

Figure 6: High magnification images of the X-Y stage speed experiment (Zone B) after wet etching.

The final investigation before trialling the process upon Apollon cells was to test the affect of the power setting of the Nd YAG laser used for the grooving. Figure 7 shows zone C results where the power of the

laser was varied to observe the affect on surface roughness. As expected more power gives a smoother surface but the depth of the trench increased by approximately 0.5µm for a 1% increase in laser power.

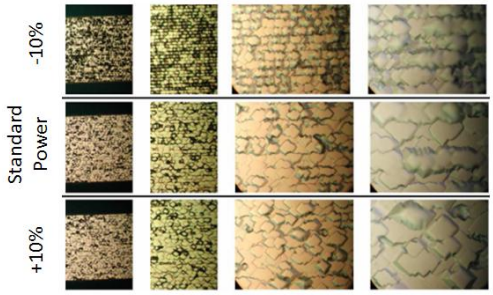

Figure 7: High magnification images of the laser power experiment (Zone C) after wet etching.

Based on the above findings a further trial was performed to deliberately produce solid bus bar cells with extremes of surface roughness, assuming that altering the conditions at the bottom of the trench that there would be a correlating difference on the surface once electroless plating steps were completed. All cells received identical processing through the standard Narec LGBC production line on all non-laser grooving steps. Ten wafers per bus bar type were produced to provide sufficient samples for testing. The trial consisted of the following three groups of cells produced using the laser parameters outlined in table 2:

i. a standard 8 groove bus bar (APPG)
ii. a rougher solid bus bar (APPR)
iii. a smoother solid bus (APPS)

Parameter Description	Standard Apollon Bus Bar APPG	Solid Bus Bar (Rough) APPR	Solid Bus Bar (Smooth) APPS
Groove Gap (mm)	Standard	Standard ÷ 5	Standard ÷ 7
Groove Qty	Standard	Standard x 4.5	Standard x 6
Laser Power	Standard	Standard	Standard + 10%
Stage Speed	Standard	Standard + 20%	Standard

Table 2: Bus bar types used on the Apollon Cell production run.

Figure 8 shows the three different bus bar types at various magnifications at the post-laser clean step. The horizontal lines are the grooves for the cell fingers while the vertical lines are the grooves for the cell bus bars. The surface roughness difference can clearly be seen between the rough and the smooth samples. Figure 9 shows the smooth and rough distinction is again still apparent after electroless plating.

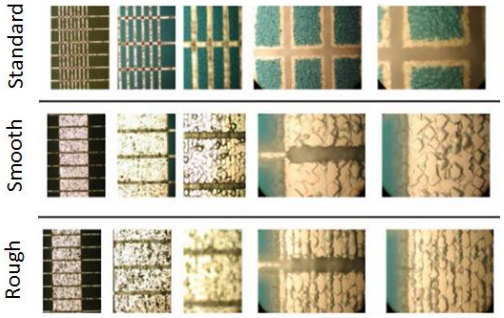

Figure 8: Images at increasing magnification of the three bus bar types on Apollon cells (pre-plating)

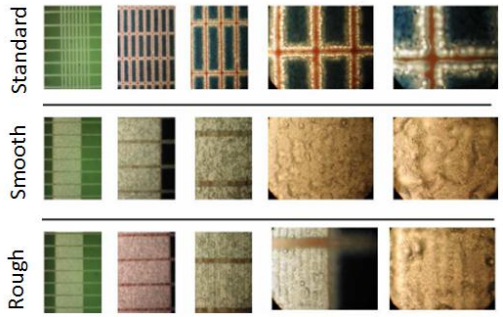

Figure 9: Images at increasing magnification of the three bus bar types on Apollon cells (post-plating)

Contact Adhesion

As an initial gauge of the bond ability of the modified bus bar several samples of each type of bus bar were strung and soldered with two different types of tabbing wire. The adhesion bond strength was then tested with Narec's in house pull test equipment.

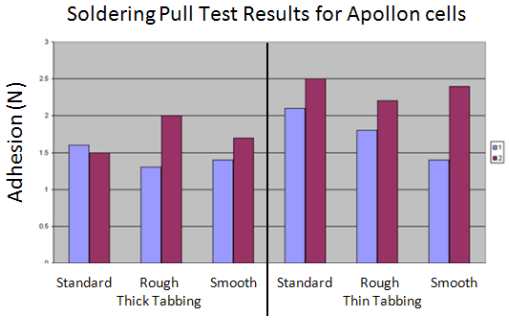

Figure 10: Soldering pull test results from cells tabbed with the thin and thick tabbing wire

Two samples per bus bar type were tested and pulled to breaking point and the pull strength point at breakage measured (in

Newtons). Figure 10 shows the results. In all cases, the rough and smooth solid bus bars were similar to the standard bus bar.

Wire Bonding Results

Cells were provided to Welwyn Components Limited in order to perform wire bond test measurements. Narec supplied three types of cell for evaluation labelled AW, BW, CW, examples of which are shown in figure 11.

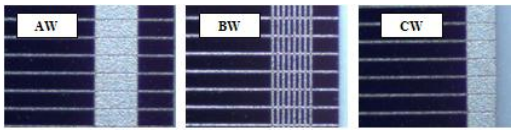

Figure 11: Images of the three groups of cells supplied for wire bonding evaluation. Smooth solid bus bar (AW), standard groove bus bar (BW) and rough solid bus bar (CW).

125µm diameter aluminium wire was chosen to fit the bus bar. Whilst the actual wire diameter is not critical for evaluation of the bond and it's degradation during accelerated life tests, the actual bond strength is dependent on the diameter of the wire. The MIL standard lower limits for pull strength for this wire diameter is 24grams, the typical breaking load of the wire is between 100 and 150grams. Bond parameters were established to give typical pull strengths for 125µm diameter aluminium wire, with correct bond deformation to MIL STD 883 and to achieve a wire break as the failure mode. The wire used was C83300145 Heraeus 125µm Lot No.1745.

After the bonding parameters were established some initial bonding and pull testing was carried out on type AW and CW cells. No parameters could be found to give any bond adhesion to cell type BW the standard LGBC bus bar, thus confirming the initial hypothesis that a new contact design was required for wire bonding. Initial pull strengths on samples AW and CW averaged 116gf and 113gf respectively. (Since 102gf = 1N), Initial bond strengths of approximately 1.1N, are similar but fractionally lower in magnitude to the in-house pull test tests carried out at Narec.

With the parameters established and satisfactory initial pull test results the remaining samples were wire bonded. A total of 45 bonds were performed on both the AW (smooth bus bar) and CW (rough bus bar) cells: 15 bonds were used as control samples, 15 bonds went through a high temperature storage test (96 hours storage at a temperature of 150ºC), and 15 bonds undertook a humidity test (96 hour long damp heat test at 40ºC and 93% relative humidity). After the high temperature storage and humidity testing, pull tests on all of the bonds were carried out. Table 3 shows the pull test results for the AW (smooth bus bar) and CW (rough bus bar) cells for the three groups, the control group, the group that went through the high temperature storage test and the group that undertook the humidity test.

Condition	Control		Temp. Storage		Damp Heat	
Cell Type	AW	CW	AW	CW	AW	CW
Average	122.2	118.9	108.4	117.4	110.7	115.3
Std. Dev.	12.4	8.8	13.0	12.8	11.6	7.9
Minimum	99.5	103.9	90.6	87.2	95.4	96.9
Maximum	141.2	129.6	132.7	133.5	134.7	126.3

Table 3: Pull Test results, post aging (units are in grams)

All Bonds had 1st or 2nd bond heal breaks (wire break) except the lowest value of 87.2 which was a first bond pad lift. Although the preferred failure mode is a wire break, this is well inside of the acceptable limit of 24 grams minimum, in accordance with MIL STD 883 method 2011.

Conclusions

LGBC cells with a solid planar bus bar have been produced which are appropriate to allow wire bonding. Whilst no bonding parameters could be found that would allow wire bonding to our standard bus bar, solid bus bars with both smooth and rough surface have demonstrated acceptable wire bond pull strengths, both initially and post aging.

Acknowledgements

The authors would like to thank the team at Narec PVTC and David Barrow from the Extreme laser facility at Cardiff University for the interferometric surface profile shown in figure 3. This work was partially funded by the European Commission in the FP7 funded APOLLON project (Grant number 213514).

References

[1] www.apollon-eu.org 20th February 2010